International Journal of Osteoporosis & Metabolic Disorders

ISSN 1994-5442

science alert

ANSInet
an open access publisher
http://ansinet.com

OPEN ACCESS International Journal of Osteoporosis and Metabolic Disorders

ISSN 1994-5442
DOI: 10.3923/ijom.2016.1.12

Research Article
Low Bone Mass Estimation: The Exhibition of Semi-automated Approach over the Manual Method in a Comparative Perspective With DXA

D. Ashok Kumar and M. Anburajan

Department of Biomedical Engineering, SRM University, Kattankulathur, 603203 Chennai, Tamil Nadu, India

Abstract

Background: Osteoporosis is an ailment with decremented quality and density of the bone. Bone mineral density measurements were performed by dual energy x-ray absorptiometry (DXA) which is used in the diagnosis of osteoporosis. **Objective:** The main objectives of the study are (i) To evaluate low bone mass in South Indian women by means of Fuzzy Local Information Clustering Means (FLICM) with respect to diagnosis of low BMD in a comparative perspective with DXA. (ii) To Assess the capability of manual as well as CAD measurements in the evaluation of osteoporosis. **Methodology:** In this study an semi-automated Computer Aided Diagnosis (CAD) system for osteoporotic risk detection using digital radiographs was presented. The radiograph was intensified, the measured bone indicies such as periosteal and endosteal width were measured and the femur shaft cortical thickness (FS-CCT_{SA}) and percentage cortical thickness of femur shaft FS-CCT_{SA}(%) was calculated. Combined cortical thickness of femur shaft has been used in the derived regression formula to predict total hip BMD (T.BMD) and compared with T.BMD by DXA. **Results:** The combined cortical thickness of femur shaft of total studied population and the old aged population was strongly correlated ($p<0.01$) with DXA femur T.BMD measurements. The empirical formula was identified as a better tool for predicting low bone mass in total population and old-aged population with a sensitivity (85.7 and 94.7%), specificity (86.6 and 87.5%), positive predictive value (90 and 94.7%) and negative predictive value (81.2 and 87.5%), respectively. **Conclusion:** The results suggest that the derived empirical formula is useful and better index than other simple radiogrammetry measurements in the evaluation of low bone mass. An automated CAD tool could be implemented by involving standard conventional digital x-rays of other skeletal sites, namely clavicle and forearm will be useful as a cost effective mass screening tool in the evaluation of low bone mass.

Key words: Radiogrammetry, osteoporosis, FLICM, FS-CCT, CAD, DXA, BMD

Received: May 07, 2016 Accepted: May 30, 2016 Published: June 15, 2016

Citation: D. Ashok Kumar and M. Anburajan, 2016. Low bone mass estimation: The exhibition of semi-automated approach over the manual method in a comparative perspective with DXA. Int. J. Osteoporosis Metab. Disorders, 9: 1-12.

Corresponding Author: M. Anburajan, Department of Biomedical Engineering, SRM University, Kattankulathur, 603203 Chennai, Tamil Nadu, India
Tel: +919790840279

Competing Interest: The authors have declared that no competing interest exists.

Data Availability: All relevant data are within the paper and its supporting information files.

INTRODUCTION

Osteoporosis is a metabolic bone disorder characterized by reduced bone mass and deterioration of bone architecture[1]. Bone fragility and susceptibility to a fracture are increased due to resorption of bone[2-5]. The clinical diagnosis of osteoporosis is typically based on the measurements of bone mineral content/density (BMC/BMD) by dual-energy x-ray absorptiometry (DXA)[6].

Over the last few decades, several studies have been reported toward understanding the role of cortical bone properties in determining the status of bone health and efficacy of treatment. Cortical bone properties, such as BMD and cortical bone thickness have been proved to be highly related to bone turnover under bone diseases such as osteoporosis[7,8].

The process which contributing to bone loss is a decrease in cortical bone, mainly caused by increased porosity from both an increase in resorption cavities and an accumulation of incompletely closed osteons with aging[9]. The mid-diaphyseal femoral cortex has shown clear and predictable patterns of porosity changes with increasing 'biological age' and distinct sex differences in this process, a process that ultimately leads to cortical thinning[10].

The BMD of the hip actually refers to the femoral neck BMD or total hip BMD in which the total hip BMD has better precision than femoral neck BMD[11]. Cortical thickness of the proximal femur shaft decreases with age[12]. The subtrochanteric fractures are a subcategory of diaphyseal fractures, occurring within 3 cm below the lesser trochanter[13].

Radiography can be used to analyze both trabecular structure and bone geometry and information on bone density may be obtained using appropriate image analysis techniques[14]. From the hip geometry, the manual cortical femoral diaphysis approximates a cylindrical beam and its geometric properties can be calculated from measurements of cortical dimensions to give evaluations of bone quality in addition to those derived from bone mineral measurements[15]. Napoli *et al.*[16] studied the outlines of the inner and outer edge of the four cortices of the proximal femur shaft (medial and lateral, left and right) were measured from the lesser trochanter and using the image J (Image processing and analysis using java) software, the bilateral medial and lateral cortical width were calculated. Finite Element Analysis (FEA) of hip fracture model using CT image is a promising tool to enhance the prediction of future osteoporotic fracture risk in people[17,18].

An algorithm was developed to evaluate the femur Cortical Bone Thicknesses (CBT) from the areal bone mineral density (aBMD) profile of the cross-section at the medial (inferior) side and the lateral (superior) side from clinical hip DXA[19]. The endocortical diameters and cortical thicknesses were assesed by utilizing the estimations of cross-area and the mean cortical thicknesses which is based on a structural model of the hip[20].

In India, the assecebility of DXA machines is limited and the cost is also very high, so mostly radiographs are preferred in diagnosis purpose due to it's low cost and it can be affordable to common people.

The main objectives of this study were listed as follows: (i) To develop semi automated computer diagnostic approach for the measurement of femoral shaft cortical thickness in the evaluation of low bone mass and (ii) To establish an empirical formula to predict total hip BMD (g cm^{-2}) using simple femoral shaft radiogrammetry with good accuracy.

MATERIALS AND METHODS

Subjects: The study is an approach related to osteoporosis within the framework of public health. A free screening camp for osteoporosis was organized in 2010, in collaboration with the SRM Hospital and Medical Research Centre, SRM University, Kattankulathur, Chennai, India. The Department of Health Care Ethics, SRM University approved the study protocol after careful evaluation. Subjects provided necessary information through a self prepared questionnaire concerning a wide range of general health and socioeconomic factors.

In this study, 36 South Indian pre-menopausal and post-menopausal women, whose age ranged from 30-90 years (Mean$\pm$SD age = 52.83$\pm$12.94 years) were participated. None of them had chronic illnesses significantly impairing their functional ability or recognized disorders of calcium metabolism. Also none had a history of alcohol abuse or drugs which would have a negative impact on bone. The ratio of body weight in kilogram to the square of body height in meter was used to calculate Body Mass Index (BMI).

Mesurements

Proximal femur DXA scan: The BMD (g cm^{-2}) at the right proximal femur of each woman was measured by a standard DXA bone densitometer (DPX prodigy, DXA scanner, GE-lunar corp., USA) using standard protocol by a well trained radiographer with good experience. The BMD at following regions of interest were measured quantitatively by the dedicated software provided by the manufacturer: (1) Neck region (N.BMD), (2) Ward's triangle (W.BMD), (3) Trochanter (Tr.BMD), (4) Shaft (S.BMD) and (5) Total hip (T.BMD). The T.BMD was considered for the diagnosis of osteoporosis in the total study population.

Digital right hip x-ray: In each woman, a standard digital right hip anterior-to-posterior (AP) view x-ray was taken using the x-ray machine referred with an x-ray tube voltage and tube current of 25-30 Kvp and 25-30 mAs, respectively at film tube distance of 100 cm. While taking x-ray the right femur was rotated internally by 15°.

Study groups: The following approaches were used to subdivide the total women studied:

- **Approach-I:** Based on subject's (age), women were sub-divided into two groups as follows:
  - **Group-I:** Young women, aged less than 50 years (n = 9, Mean±SD age = 36±5.52 years)
  - **Group-II:** Older women, aged 50 years and above (n = 27, Mean±SD age = 58.44±9.22 years)
- **Approach-II:** Out of various ROI's of DXA scan in the proximal femur, T.BMD (g cm^{-2}) was used in this study for classifying the women according to WHO's diagnostic criteria (1994) for osteoporosis. The classification by T-score was carried out using a measured mean value of 1.052 (g cm^{-2}) and apopulation SD of 0.152 (g cm^{-2}) for T.BMD in young normal women aged 25-35 years[21]. Using the diagnostic criteria, women were divided into two groups as follows:
  - **Group-I:** Normal (those with T-score≥-1) (n = 15, Mean±SD age = 45.6±10.74 years)
  - **Group-II:** Low bone mass (those with T-score above-1), (n = 21, Mean±SD age = 58±12.04 years)

Digital image analysis

Manual approach: The manual measurement of femur shaft was done by DICOM viewer which was used to analyze the digital hip x-ray. The right hip x-ray region of interest was estimated at 3 cm below the lesser trochanter were measured using a ruler tool with an accuracy of 0.01 mm. At the region of interest the femoral periosteal shaft width (FSW_M) and femoral endosteal shaft width (Fsw_M) were measured manually using dicom viewer separately[21]. From these measurements the following bone mass indices were calculated as follows:

- Combined cortical thickness of femur shaft $FS\text{-}CCT_M = (FSW_M\text{-}Fsw_M)$
- Percentage of combined cortical thickness of femur shaft $FS\text{-}CCT_M$ (%) = $(FSW_M\text{-}Fsw_M/FSW_M)\times 00$

Semi-automated approach: The acquired right proximal femur images are stored in DICOM (digital imaging and communications in medicine) format. The detailed flow diagram of the proposed CAD system is shown in Fig. 1.

Edge detection and clustering are the two basic segmentation methods among the various techniques. Edge detection is to identify the image brightness discontinuities along the edges where the intensity tends to change sharply. Canny edge detection is a technique used for detecting the edge in an image. Clustering is a process where data set is replaced by clusters, which are collections of data points that "belong together". In image segmentation the image clustering is the representation of an image in terms of clusters of pixels that "belong together". The study is an enhanced form of edge detection methodology that aids to obtain the best results[22].

In this proposed system the input image is pre-processed, where the image was subject to contrast enhancement and the key point of the enhanced image is set below the lesser trochanter. Then the Region of Interest (ROI) is measured in the image is automatically cropped around the femur shaft region.

Image segmentation is a process of dividing an image into different regions such that each region is nearly homogeneous. Here the cropped image is subjected to Fuzzy Local Information Clustering Means (FLICM) segmentation algorithm were iterative clustering method will produce an optimal c partition by minimizing the weighted within group sum of squared error objective function[23].

The clustering method will have the novel fuzzy factor G_{ki} were:

$$G_{ki} = \sum_{\substack{j\in Ni \\ i\neq j}} \frac{1}{d_{ij}+1}\left(1-u_{kj}\right)^{m}\left\|x_j - v_k\right\|^2 \quad (1)$$

The factor G_{ki} is completely free of using any parameter that controls the balance between the image noise and the image details. The control of this balance is automatically achieved by the fuzziness of each image pixel (both spatial and gray level). The d_{ij} is the spatial Euclidean distance between pixels i and j and the factor G_{ki} makes the influence of the pixels within the local window to change flexibly according to their distance from the central pixel. Thus more local spatial information can be used. The important component of a clustering algorithm is the distance measure between data points.

The FLICM incorporates local spatial and gray level information into its objective function, the algorithm composed of the following steps:

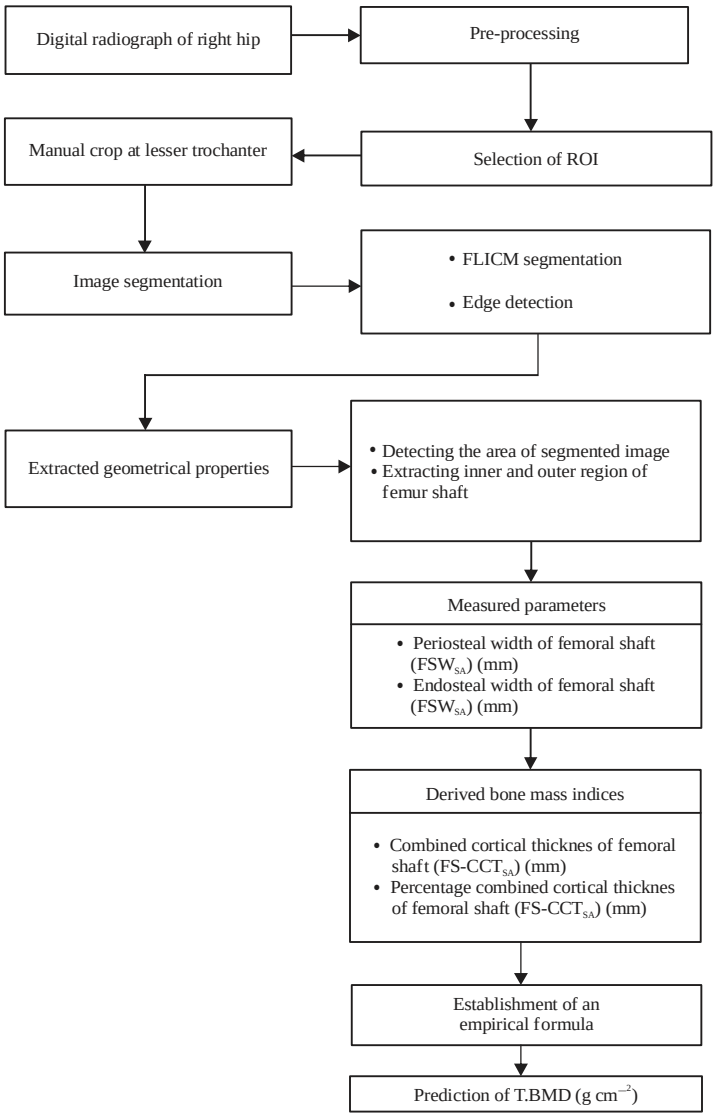

Fig. 1: Flow diagram depicting the semi-automated image analysis of right hip radiograph

Step 1: Set the number 'c' of the cluster prototypes, fuzzification parameter 'm' and the stopping condition".

Step 2: Initialize randomly the fuzzy partition matrix

Step 3: Set the loop counter b = 0.

Step 4: Calculate the cluster prototypes using the following Eq. 2 'v_k':

$$v_k = \frac{\sum_{i=1}^{N} u_{ki}^{m} x_i}{\sum_{i=1}^{N} u_{ki}^{m}} \quad (2)$$

Step 5: Compute membership values using 'u_{ki}':

$$u_{ki} = \frac{1}{\sum_{j=1}^{c} \left(\frac{\|x_i - v_k\|^2 + G_{ki}}{\|x_i - v_j\|^2 + G_{ji}} \right)^{\frac{1}{m-1}}} \quad (3)$$

Step 6: If max U (b)-U(b+1)< " then stop, otherwise, set b = b+1 and go to cluster prototype.

Then the clustering algorithm will partition the image into four clusters, the best among the four will differentiate the required outer layer and the inner core region of the femur shaft in the cropped image. The boundary tracking of the partitioned image is done by canny edge detection algorithm[24].

The algorithm process is done by following the steps:

Step 1: Smoothening the original image.
Step 2: Finding the intensity gradient level of the image.
Step 3: Apply non maxima suppression in the image.
Step 4: Apply thresholding and track the edges of the image.

This technique is applied to the best cluster where it fills the holes on the edge detected image and extracts the inner and outer portion. The extracted features from the femur shaft will calculate the binary areas of the cropped image and the following bone mass indices such as outer periosteal width femur shaft (FSW_{SA}) and the inner endosteal width of the bone (Fsw_{SA}) were measured.

From these semi-automated measured parameters the bone mass indices such as, the combined cortical thickness of femur shaft ($FS\text{-}CCT_{SA}$) and percentage of combined cortical thickness of femur shaft ($FS\text{-}CCT_{SA}$) (%) were calculated. The calculated bone mass indices and age is used to predict the T.BMD from the derived empirical formula. The technique was implanted in Mat lab software (R2012a version) which was used on the platform with windows 7 background with 4 GB of RAM.

Statistical analysis: The data was performed with the SPSS version 17.0 (SPSS Inc., Chicago, USA). Mean±SD values of the various measurements were calculated in each group/approach. Association between variables was investigated by correlation and multiple linear regression analysis. Student's t-test was used to compare the Mean±SD values of each variable between groups/approach.

RESULTS

Digital femoral shaft radiogrammetry: Figure 2 and 3 show the femoral shaft width measurement done in digital x-ray of a sample woman having low bone mass by manual and semi-automated-radiogrammetry approaches.

Statistical correlation: All women combining both normal as well as low bone mass (n = 36, Mean±SD age = 52.83±12.94 years): Table 1 shows the statistical correlation matrix between measured femoral shaft radiogrammetry variables compared with BMD variables by DXA in total study women. The T.BMD negatively correlated ($p<0.01$) with subject's age ($r = -0.61$) and positively correlated ($p<0.01$) with body weight (kg) and BMI ($r = 0.54$ and $r = 0.47$, respectively). The T.BMD measured DXA was correlated statistically significant ($p<0.01$) with the following radiogrammetry variables measured by both manual and semi-automated methods: (i) $FS\text{-}CCT_M$ ($r = 0.57$), (ii) $FS\text{-}CCT_M$ (%) ($r = 0.68$), (iii) $FS\text{-}CCT_{SA}$ ($r = 0.60$) and (iv) $FS\text{-}CCT_{SA}$(%) ($r = 0.66$). The other parameters were not significantly correlated with T.BMD.

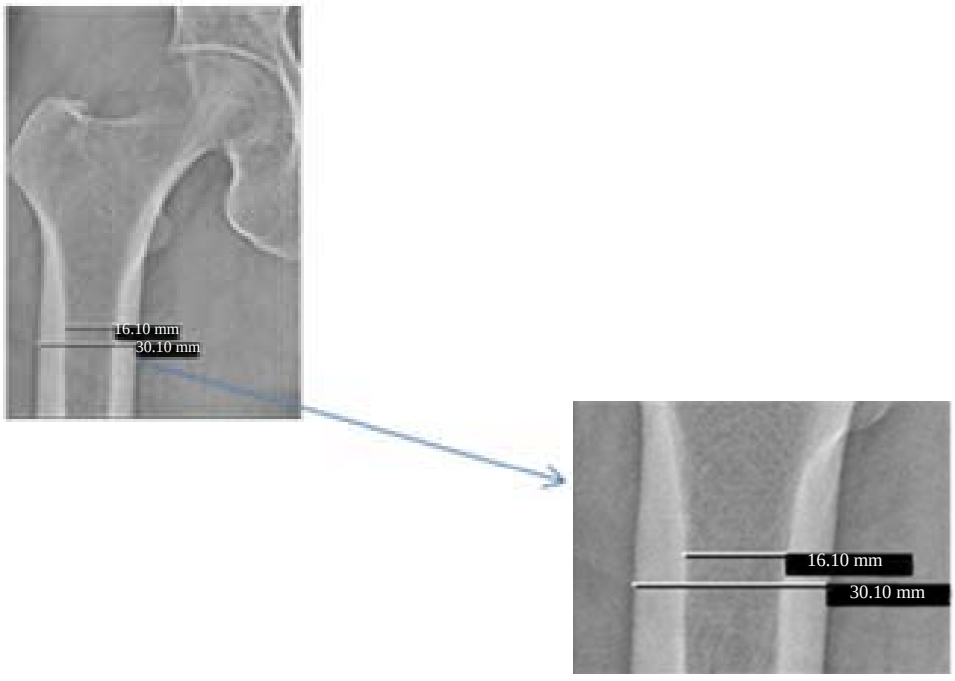

Fig. 2: Manual femoral shaft width measurement in a sample woman having low bone mass ($FSW_M = 30.10$ and $Fsw_M = 16.10$ mm)

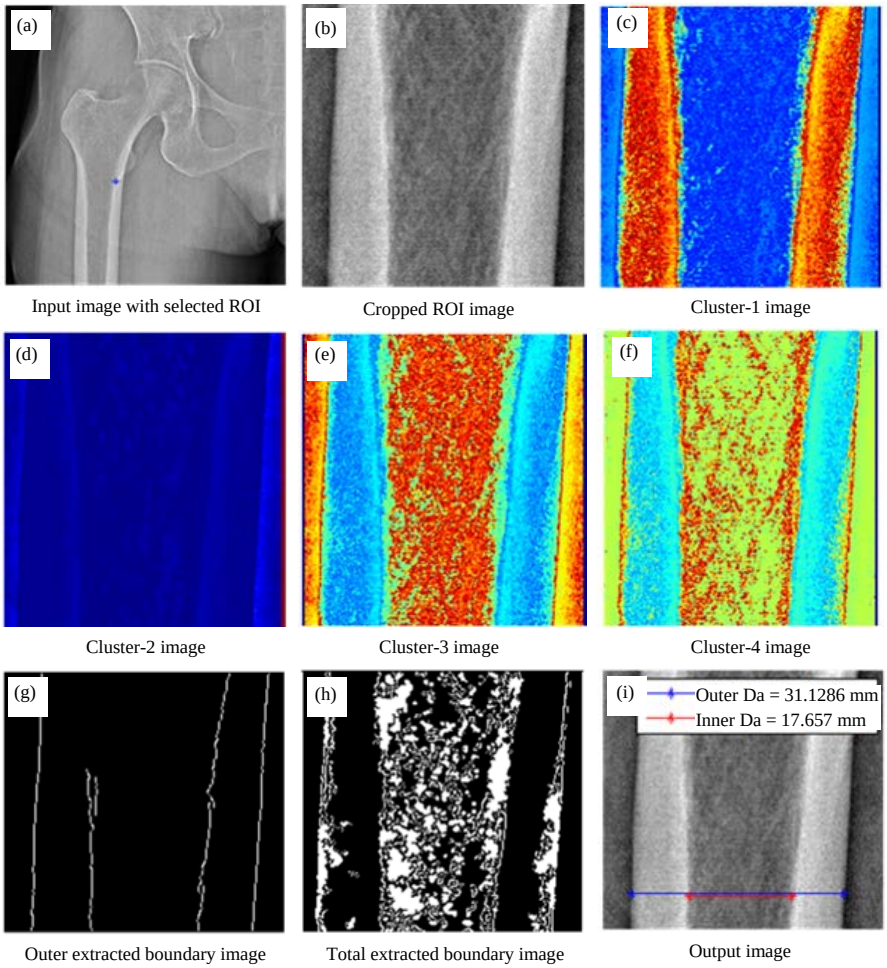

Fig. 3(a-i): Semi-automated femoral shaft width measurement in a sample woman having low bone mass, (a) Input image with selected ROI, (b) Cropped ROI image, (c) Cluster-1 image, (d) Cluster-2 image, (e) Cluster-3 image, (f) Cluster-4 image, (g) Outer extracted boundary image, (h) Total extracted boundary image and (i) output image measurements shows FSW_{SA} = 31.12 mm and Fsw_{SA} = 17.66 mm

Table 1: Correlation matrix for the different variables in total women studied (n = 36)

			DXA (Right proximal femur)				
Sl No.	Methods	Variables	N.BMD (g cm^{-2})	W.BMD (g cm^{-2})	Tr.BMD (g cm^{-2})	S.BMD (g cm^{-2})	T.BMD (g cm^{-2})
I	Demographic features	Age (years)	-0.62**	-0.61**	-0.55**	-0.59**	-0.62**
		Body height (cm)	0.32	0.20	0.15	0.21	0.22
		Body weight (kg)	0.51**	0.39*	0.46**	0.56**	0.54**
		BMI (kg m^{-2})	0.37*	0.32	0.42*	0.50**	0.47**
II (a)	Femoral shaft radiogrammetry	Directly measured					
	(Digital right hip x-ray)	FSW_M (mm)	-0.07	-0.15	-0.16	-0.14	-0.16
	Manual method	Fsw_M (mm)	-0.61**	-0.56**	-0.60**	-0.64**	-0.64**
		Calculated bone mass indices					
		$FS\text{-}CCT_M$ (mm)	0.63**	0.49**	0.53**	0.59**	0.57**
		$FS\text{-}CCT_M$ (%)	0.71**	0.59**	0.63**	0.69**	0.68**
II (b)	Femoral shaft radiogrammetry	Directly measured					
	(Digital right hip x-ray)	FSW_{SA} (mm)	-0.01	-0.07	-0.06	-0.05	-0.07
		Fsw_{SA} (mm)	-0.52**	-0.50**	-0.55**	-0.56**	-0.57**
	Semi-automated method	Calculated bone mass indices					
		$FS\text{-}CCT_{SA}$ (mm)	0.62**	0.52**	0.58**	0.61**	0.60**
		$FS\text{-}CCT_{SA}$ (%)	0.66**	0.59**	0.64**	0.67**	0.66**

Values represented are pearson's correlation coefficient®, **p<0.01, *p<0.05, All women (combining both normal and who are at low bone mass, n = 36, Mean±SD age = 52.83±12.94 years)

Table 2: Correlation matrix for the different variables studied in older women aged above 50 years (n = 27)

			DXA (Right proximal femur)				
Sl No.	Methods	Variables	N.BMD (g cm^{-2})	W.BMD (g cm^{-2})	Tr.BMD (g cm^{-2})	S.BMD (g cm^{-2})	T.BMD (g cm^{-2})
I	Demographic features	Age (years)	-0.53**	-0.49**	-0.51**	-0.52**	-0.55**
		Body height (cm)	0.32	0.19	0.16	0.20	0.21
		Body weight (kg)	0.60**	0.48**	0.52**	0.64**	0.61**
		BMI (kg m^{-2})	0.44*	0.41*	0.46*	0.57**	0.53**
II (a)	Femoral shaft radiogrammetry	Directly measured					
	(Digital right hip x-ray)	FSW_M (mm)	-0.10	-0.19	-0.20	-0.17	-0.19
		Fsw_M (mm)	-0.71**	-0.65**	-0.69**	-0.70**	-0.71**
	Manual method	Calculated bone mass indices					
		$FS\text{-}CCT_M$ (mm)	0.67**	0.51**	0.54**	0.59**	0.58**
		$FS\text{-}CCT_M$ (%)	0.79**	0.66**	0.70**	0.73**	0.74**
II (b)	Femoral shaft radiogrammetry	Directly measured					
	(Digital right hip x-ray)	FSW_{SA} (mm)	-0.05	-0.14	-0.14	-0.10	-0.13
		Fsw_{SA} (mm)	-0.69**	-0.64**	-0.69**	-0.68**	-0.70**
	Semi-automated method	Calculated bone mass indices					
		$FS\text{-}CCT_{SA}$ (mm)	0.69**	0.569**	0.619**	0.64**	0.63**
		$FS\text{-}CCT_{SA}$ (%)	0.78**	0.68**	0.73**	0.75**	0.75**

Values represented are pearson's correlation coefficient®, **p<0.01, *p<0.05, older women aged above 50 years (n = 27; Mean±SD age = 58.44±9.22 years)

Table 3: Statistical differences in demographic features, DXA and radiogrammetry parameters between normal and low bone mass

Sl No.	Methods	Group I Variables	Group II Normal (n = 15)	Low bone mass (n = 21)	Statistical significance (p-value)
I	Demographic features	Age (years)	45.60±10.74	58.00±12.04	0.003**
		Body height (cm)	151.33±5.68	148.29±6.10	0.138
		Body weight (kg)	57.67±9.76	50.24±7.60	0.015*
		MI (kg m^{-2})	25.00±4.22	22.82±2.95	0.076
II	DXA (Right proximal femur)	N.BMD (g cm^{-2})	0.98±0.07	0.70±0.10	0.000***
		W.BMD (g cm^{-2})	0.83±0.09	0.51±0.11	0.000***
		Tr.BMD (g cm^{-2})	0.81±0.08	0.53±0.11	0.000***
		S.BMD (g cm^{-2})	1.25±0.09	0.83±0.17	0.000***
		T.BMD (g cm^{-2})	1.04±0.08	0.69±0.13	0.000***
III (a)	Femoral shaft radiogrammetry	Directly measured			
	(Digital right hip x-ray)	FSW_M (mm)	30.90±2.93	30.89±2.45	0.998
		Fsw_M (mm)	14.94±2.56	17.57±2.77	0.007**
	Manual method	Calculated bone mass indices			
		$FS\text{-}CCT_M$ (mm)	15.96±2.66	13.33±1.90	0.001**
		$FS\text{-}CCT_M$ (%)	51.62±6.83	43.28±6.22	0.001**
III (b)	Femoral shaft radiogrammetry	Directly measured			
	(Digital right hip x-ray)	FSW_{SA} (mm)	32.07±2.87	31.43±2.77	0.506
		Fsw_{SA} (mm)	16.66±2.80	19.24±3.04	0.014*
	Semi-automated method	Calculated bone mass indices			
		$FS\text{-}CCT_{SA}$ (mm)	15.40±2.62	12.19±1.82	0.000***
		$FS\text{-}CCT_{SA}$ (%)	48.07±6.86	38.98±6.09	0.000***
IV	Semi-automated CAD for evaluation ($Y = 0.645\text{-}0.007\ (X_1)+0.013\ (X_2)+0.009\ (X_3)$)	Predicted T.BMD (g cm^{-2})	0.96±0.09	0.75±0.13	0.000***

Significance by unpaired student's t-test, ***p<0.001, **p<0.01, *p<0.05

Older women aged 50 years and above (n = 27, Mean±SD age = 45.6±10.74 years) Table 2 shows the statistical correlation matrix between measured femoral shaft radiogrammetry variables compared with DXA, in women aged above 50 years. The T.BMD negatively correlated (p<0.01) with subject's age (r = -0.55) and positively correlated (p<0.01) with body weight (kg) and BMI (r = 0.61 and r = 0.53, respectively). The T.BMD measured DXA was correlated statistically significant (p<0.01) with the following radiogrammetry variables measured by manual and semi-automated-methods: (i) $FS\text{-}CCT_M$ (r = 0.58), (ii) $FS\text{-}CCT_M$(%) (r = 0.74), (iii) $FS\text{-}CCT_{SA}$ (r = 0.63) and (iv) $FS\text{-}CCT_{SA}$(%) (r = 0.75). The other parameters were not significantly correlated.

Comparison between low bone mass and normal women: Table 3 which shows the statistical differences in demographic features, DXA and radiogrammetric parameters

between normal group (n = 15) and low bone mass group (n = 21). The mean age of women in normal and low bone mass groups were 45.60±10.74 and 58.00±12.04 years respectively. In low bone mass group the measured body weight (kg) were lesser by 12% [(57.67-50.64)/57.67×100] compared to normal group, which was statistically significant ($p<0.05$). The measured BMD by DXA at various regions of interest of the proximal femur were lesser significantly in low bone mass group compared to normal group. Bone density was significantly lower in the low bone mass group compared to the normal group with a reduction of 34% for T.BMD and 29% for N.BMD ($p<0.001$) and manual calculated bone mass indices of femur shaft with a reduction of 16% for FS-CCT_M and FS-CCT_M (%) ($p<0.01$). In semi automated calculated bone mass indices of femur shaft the bone density was significantly lower in low bone mass group compared to the normal group, with a reduction of 21% for FS-CCT_{SA} and 19% for FS-CCT_{SA} (%) ($p<0.001$). The predicted T.BMD low bone mass group were lesser by 22% compared to normal group which were statistically significant ($p<0.001$). The other parameters were not significant.

Establishment of empirical formula: Based on the step-wise regression model, the following empirical formula was established by combining the subject's age (years) and the extracted both CCT and percentage CCT of the femoral shaft:

$$Y = 0.645-0.007\ (X_1)+0.013\ (X_2)+0.009\ (X_3) \quad (4)$$

Where:
Y = Predicted total hip BMD (T.BMD) (g cm^{-2})
X_1 = Patient's age
X_2 = CCT (mm) of the femoral shaft
X_3 = Percentage CCT of the femoral shaft

In both total women (n = 36) and older women aged 50 years and above (n = 27), the predicted T.BMD using the established formula was correlated statistically significant ($p<0.01$) with T.BMD by DXA (r = 0.79 and r = 0.82, respectively). Figure 4 shows statistically significant supportive relationship between the predicted T.BMD and estimated T.BMD in total women studied ($r^2 = 0.621$, $p<0.001$) and Fig. 5 shows statistically significant supportive relationship between

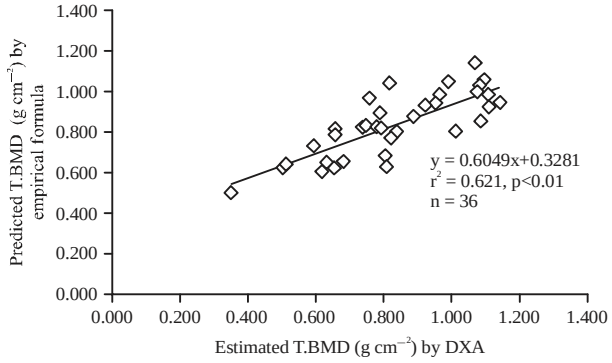

Fig. 4: Statistically significant supportive relationship between the predicted T.BMD and estimated T.BMD by DXA in total women studied

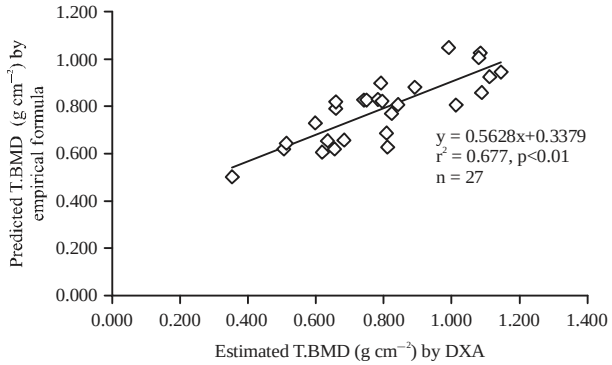

Fig. 5: Statistically significant supportive relationship between the predicted T.BMD and estimated T.BMD by DXA in older women aged above 50 years

Table 4: Validation of the predicted total hip BMD using established empirical formula among the study population (n = 36)

Women	Age (Years)	FS-CCT$_{SA}$ (mm)	FS-CCT$_{SA}$ (%)	Estimated T.BMD (g cm^{-2}) by DXA	Predicted T-BMD (g cm^{-2})	Test	Women	Age (Years)	FS-CCT$_{SA}$ (mm)	FS-CCT$_{SA}$ (%)	Estimated T.BMD (g cm^{-2}) by DXA	Predicted T-BMD (g cm^{-2})	Test
1	26	15.80	52.90	1.071	1.144	TN	19	65	10.79	35.69	0.634	0.652	TP
2	35	13.47	45.37	0.966	0.983	TN	20	56	15.97	51.62	1.113	0.925	TN
3	35	13.11	40.28	0.927	0.933	TN	21	53	13.96	41.20	0.782	0.826	TP
4	36	15.97	49.06	0.818	1.042	FN	22	57	12.93	39.51	0.822	0.770	TP
5	39	12.40	35.01	1.087	0.848	FP	23	71	11.15	36.24	0.654	0.619	TP
6	40	13.08	48.48	0.761	0.971	FN	24	54	18.30	57.80	1.084	1.025	TN
7	32	14.01	42.57	1.110	0.986	TN	25	52	12.76	39.41	1.013	0.802	FP
8	35	15.79	50.45	1.097	1.059	TN	26	80	13.65	39.54	0.506	0.618	TP
9	46	14.73	47.87	0.957	0.945	TN	27	52	9.00	27.05	0.514	0.641	TP
10	70	10.43	37.38	0.811	0.627	TP	28	56	20.45	58.93	0.991	1.049	TN
11	57	16.52	46.40	0.892	0.878	TN	29	52	12.83	40.99	0.660	0.817	TP
12	60	13.47	43.04	0.660	0.787	TP	30	76	11.68	37.75	0.620	0.605	TP
13	55	9.72	38.00	0.596	0.728	TP	31	57	10.07	30.77	0.683	0.654	TP
14	51	12.10	40.17	0.841	0.807	TP	32	51	11.86	46.04	1.090	0.857	TN
15	81	11.33	30.60	0.351	0.501	TP	33	55	19.92	53.53	1.080	1.001	TN
16	50	9.71	29.19	0.807	0.684	TP	34	55	15.98	52.86	1.144	0.943	TN
17	60	14.73	45.49	0.750	0.826	TP	35	50	13.29	47.63	0.790	0.896	FN
18	52	12.47	41.50	0.794	0.817	TP	36	50	13.55	39.25	0.742	0.824	TP

TP: Truepositive, TN: Truenegative, FP: Falsepositive and FN: Falsenegative

the predicted T.BMD and estimated T.BMD in older women aged above 50 years ($r^2 = 0.677$, $p<0.001$).

Validation of empirical formula: All women combining both normal as well as low bone mass were tested with the established empirical formula which shows the validation test results the total studied population (n = 36) indicated that sensitivity (85.7%), specificity (86.6%), Positive Predictive Value (PPV) (90%) and Negative Predictive Value (NPV) (81.2%) were achieved and shown in Table 4.

Older women aged 50 years and above (n = 27) were tested using the established empirical formula in which the validation test results indicated that sensitivity (94.7%), specificity (87.5%), Positive Predictive Value (PPV) (94.7%) and Negative Predictive Value (NPV) (87.5%) were achieved and the same was shown in supplementary 3 (Sl No. 10-36).

DISCUSSION

Osteoporosis which has been witnessed to be a menace in epidemiological frame work has to be controlled and also to be diagnosed in the earlier phase itself. Keeping in view this prime aspect, the present article aims at providing a computer aided diagnostic method to access osteoporosis in a précised manner.Aging affects cortical thickness by increasing endocortical bone resorption and reducing periosteal apposition[25]. The body weight or BMI has been found to be inversely related to the risk of osteoporotic fracture[26,27].

Women lose bone at a faster rate than men, over aging[28,29]. The CCT decreases with age in both the genders, especially in older group. There is a gradual thinning of the cortex of the radius with age in both sexes to a greater extent in females than in males[30]. The main limitation of cortical thickness as an indication of osteoporosis is that, since it is a continuous variable, it is not possible to give a precise level at which normality ends and abnormality begin[31].

In contiguity with our discussion, a similar cohort (n = 52) arranged by Yao *et al.*[32] in which the manual measurements were compared with semi-automated once, it exhibited the statistical accuracy at the level of ($p<0.001$). In our study the comparative perspective between manual and semi automated quantifications evidenced the statistical significance at the level of ($p<0.01$). Morar *et al.*[33] advocated an image processing algorithm in order to detect lesser trochanter by means of a circle, which shows 50% accuracy depicted in comparison with manual detection. But in this study as stated above the image processing methodology (semi automated) exhibited higher precision with respect to manual gauges, here the algorithm (FLICM and canny method) automatic detection of the lesser trochanter is done efficiently and also it detects the exact region of interest of periosteal and endosteal width of the femoral shaft.

In his study on femoral shaft cortex Gluer *et al.*[34] endorsed the utilization of independent methodology for hip fracture prediction on the basis of reduced cortical thickness of the femoral shaft cortex. In this study FS-CCT exhibited lesser significance of 16 and 21% with respect to manual and semi automated measurements compared to low bone mass group. In addition to the BMD measurements at T.BMD and N.BMD demonstrated lesser significance of 34 and 29%, respectively against normal group by low bone mass group.

The study of measurement method of comparison data, the correlation coefficient techniques such as regression analysis are suitable for evaluation in low bone mass[35]. In the present study a similar type of agreement for the measurement of cortical thickness with age using regression analysis for the prediction of T.BMD due to high precision than other measured DXA variables.

Riggs *et al*.[36] found the direct proportionality between onset of menopause and loss of bone mass. Likewise this study also detailed the similar information (degree of agreement between FS-CCT (r = 0.62) and BMI (r = 0.52), FS-CCT and BMI implies the correlation of reduced bone loss with lower BMI.

Kumar and Anburajan[21] proclaimed that in low bone mass group the values of FS-CCT and FS-CCT (%) of hip to be fewer by 15 and 13% compared to normal group. In the present study semi-automated methodology manifested the values of $FS\text{-}CCT_{SA}$ and $FS\text{-}CCT_{SA}$ (%) of hip to be fewer by 21 and 19% with significance of ($p<0.001$), where a normal group was compared with low bone mass group. However, the significance level confined to ($p<0.01$) between $FS\text{-}CCT_{M}$ and $FS\text{-}CCT_{M}$ (%)[21].

In this study, it was found that 70.3% (19/27) of the South Indian old aged women were diagnosed to be low bone mass, based on DXA hip measurements. A related study shows that 20.7% (6/29) and 58.6% (17/29) of south Indian postmenopausal women were diagnosed to posses osteopenia and osteoporosis based on DXA hip measurements and their age ranged from 52-82 years, respectively[37].

A study on shoulder radiographs by Mather *et al*.[38] revealed that the cortical bone thickness is measured by two techniques, the gauge and the average method. It demonstrated a strong correlation with femur BMD by DXA ($r = 0.64$, $p<0.0001$). The threshold value for the cortical thickness measurement was established to predict osteoporosis, which has a sensitivity of 93%, specificity of 52% and negative predictive value[38] of 95%.

A similar kind of study was done using cortical thickness of metacarpal index which correlated significantly with DXA-BMD at the measured sites and particularly with that of the distal radius ($r = 0.67$, $p<0.0001$)[39].

In this study the total women (n = 36) and older women aged 50 years and above (n = 27), the predicted T.BMD using the established formula was correlated statistically significant ($p<0.01$) with T.BMD by DXA ($r = 0.79$ and $r = 0.82$ respectively). The established empirical formula demonstrated with a sensitivity (85.7 and 94.7%), specificity (86.6 and 87.5%), positive predictive value (90 and 94.7%) and negative predictive value (81.2 and 87.5%), in total population and old-aged population, respectively. Therefore, the proposed method could be useful in the evaluation of low bone mass in low cost environment.

The present study evidenced that 30% of South Indian old aged women age ranged from 50-81 years were in a normal phase. There is an need to make out the subjects who are in danger to osteoporotic risk, it is necessary to recommend them for osteoporotic screening and to identify a screening tool which would work on bulk databases at affordable cost[40].

CONCLUSION

The developed algorithm using the FLICM and canny edge detection method will be useful in the measurement of cortical thickness in femoral shaft and the established empirical formula involving conventional femoral shaft radiogrammetry will be useful in evaluation of low bone mass. This method would reduce the manual error and thereby increase its accuracy significantly. Moreover, it can be tested with even a person with minimum computer knowledge. The development of an automated CAD tool involving standard conventional digital x-rays of other skeletal sites, namely clavicle and forearm could be useful as a cost effective mass screening tool in the evaluation of low bone mass. Thereby, it could be used as a cost effective screening tool for the diagnosis of osteoporosis with high accuracy, especially in India due to non availability of DXA machines.

ACKNOWLEDGMENTS

The authors wish to express their gratitude to the health care authorities of SRM Hospital and Research Centre and Faculty of Engineering and Technology, SRM University for providing the required facilitative infrastructure.

REFERENCES

1. Kirmani, S., D. Christen, G.H. van Lenthe, P.R. Fischer and M.L. Bouxsein *et al*., 2009. Bone structure at the distal radius during adolescent growth. J. Bone Miner Res., 24: 1033-1042.
2. Legrand, E., D. Chappard, C. Pascaretti, M. Duquenne and S. Krebs *et al*., 2000. Trabecular bone microarchitecture, bone mineral density and vertebral fractures in male osteoporosis. J. Bone Mineral Res., 15: 13-19.
3. Hudelmaier, M., A. Kollstedt, E.M. Lochmuller, V. Kuhn, F. Eckstein and T.M. Link, 2005. Gender differences in trabecular bone architecture of the distal radius assessed with magnetic resonance imaging and implications for mechanical competence. Osteoporosis Int., 16: 1124-1133.

4. Chappard, C., B. Brunet-Imbault, G. Lemineur, B. Giraudeau, A. Basillais, R. Harba and C.L. Benhamou, 2005. Anisotropy changes in post-menopausal osteoporosis: Characterization by a new index applied to trabecular bone radiographic images. Osteoporosis Int., 16: 1193-1202.
5. Benhamou, C.L., S. Poupon, E. Lespessailles, S. Loiseau and R. Jennane *et al*., 2001. Fractal analysis of radiographic trabecular bone texture and bone mineral density: Two complementary parameters related to osteoporotic fractures. J. Bone Miner. Res., 16: 697-704.
6. Anonymous, 1994. Assessment of fracture risk and its application to screening for postmenopausal osteoporosis. Report of a WHO study group. World Health Organ. Tech. Rep. Ser., 843: 1-129.
7. Nishiyama, K.K., H.M. Macdonald, H.R. Buie, D.A. Hanley and S.K. Boyd, 2010. Postmenopausal women with osteopenia have higher cortical porosity and thinner cortices at the distal radius and tibia than women with normal aBMD: An *in vivo* HR-pQCT study. J. Bone Miner. Res., 25: 882-890.
8. Burghardt, A.J., G.J. Kazakia, M. Sode, A.E. de Papp, T.M. Link and S. Majumdar, 2010. A longitudinal HR-pQCT study of alendronate treatment in postmenopausal women with low bone density: Relations among density, cortical and trabecular microarchitecture, biomechanics and bone turnover. J. Bone Miner. Res., 25: 2558-2571.
9. Chen, H., X. Zhou, H. Fujita, M. Onozuka and K.Y. Kubo, 2013. Age-related changes in trabecular and cortical bone microstructure. Int. J. Endocrinol., Vol. 2013. 10.1155/2013/213234.
10. Thomas, C.D.L., S.A. Feik and J.G. Clement, 2005. Regional variation of intracortical porosity in the midshaft of the human femur: Age and sex differences. J. Anat., 206: 115-125.
11. Cummings, S.R., F. Cosman and S.A. Jamal, 2002. Osteoporosis: An Evidence-Based Guide t o Prevention and Management. 1st Edn., ACP Press, USA., ISBN-13: 978-0943126951, pp: 29-58.
12. Koeppen, V.A., J. Schilcher and P. Aspenberg, 2012. Atypical fractures do not have a thicker cortex. Osteoporosis Int., 23: 2893-2896.
13. Muller, M.E., S. Nazarian, P. Koch and J.L. Schatzker, 1990. The Comprehensive Classification of Fractures of Long Bones. Spinger-Verlag, Berlin-Heidelberg, ISBN: 9783540181651, Pages: 201.
14. Pulkkinen, P., T. Jamsa, E.M. Lochmuller, V. Kuhn, M.T. Nieminen and F. Eckstein, 2008. Experimental hip fracture load can be predicted from plain radiography by combined analysis of trabecular bone structure and bone geometry. Osteoporosis Int., 19: 547-558.
15. Kiratli, B.J., A.E. Smith, T. Nauenberg, C.F. Kallfelz and I. Perkash, 2000. Bone mineral and geometric changes through the femur with immobilization due to spinal cord injury. J. Rehabil. Res. Dev., 37: 225-233.
16. Napoli, N., J. Jin, K. Peters, R. Wustrack and S. Burch *et al*., 2012. Are women with thicker cortices in the femoral shaft at higher risk of subtrochanteric/diaphyseal fractures? The study of osteoporotic fractures. J. Clin. Endocrinol. Metab., 97: 2414-2422.
17. Koivumaki, J.E.M., J. Thevenot, P. Pulkkinen, V. Kuhn, T.M. Link, F. Eckstein and T. Jamsa, 2012. CT-based finite element models can be used to estimate experimentally measured failure loads in the proximal femur. Bone, 50: 824-829.
18. Koivumaki, J.E.M., J. Thevenot, P. Pulkkinen, V. Kuhn, T.M. Link, F. Eckstein and T. Jamsa, 2012. Cortical bone finite element models in the estimation of experimentally measured failure loads in the proximal femur. Bone, 51: 737-740.
19. Long, Y., W.D. Leslie and Y. Luo, 2015. Study of DXA-derived lateral-medial cortical bone thickness in assessing hip fracture risk. Bone Rep., 2: 44-51.
20. Beck, T.J., A.C. Looker, C.B. Ruff, H. Sievanen and H.W. Wahner, 2000. Structural trends in the aging femoral neck and proximal shaft: Analysis of the third national health and nutrition examination survey dual-energy x-ray absorptiometry data. J. Bone Miner. Res., 15: 2297-2304.
21. Kumar, D.A. and M. Anburajan, 2014. The role of hip and chest radiographs in osteoporotic evaluation among south Indian women population: A comparative scenario with DXA. J. Endocrinol. Invest., 37: 429-440.
22. Gonzalez, R.C. and R.E. Woods, 2005. Digital Image Processing. 2nd Edn., Pearson Education, USA.
23. Krinidis, S. and V. Chatzis, 2010. A robust fuzzy local information C-means clustering algorithm. IEEE Trans. Image Process., 19: 1328-1337.
24. Canny, J., 1986. A computational approach to edge detection. IEEE Trans. Pattern Anal. Mach. Intell., 8: 679-698.
25. Szulc, P. and E. Seeman, 2009. Thinking inside and outside the envelopes of bone. Osteoporosis Int., 20: 1281-1288.
26. Cummings, S.R., M.C. Nevitt, W.S. Browner, K. Stone and K.M. Fox *et al*., 1995. Risk factors for hip fracture in white women. N. Engl. J. Med., 332: 767-774.
27. Porthouse, J., Y.F. Birks, D.J. Torgerson, S. Cockayne, S. Puffer and I. Watt, 2004. Risk factors for fracture in a UK population: A prospective cohort study. QJM, 97: 569-574.
28. Riggs, B.L., L.J. Melton, R.A. Robb, J.J. Camp and E.J. Atkinson *et al*., 2004. Population-based study of age and sex differences in bone volumetric density, size, geometry and structure at different skeletal sites. J. Bone Miner. Res., 19: 1945-1954.
29. Riggs, B.L., L.J. Melton III, R.A. Robb, J.J. Camp and E.J. Atkinson *et al*., 2008. A population-based assessment of rates of bone loss at multiple skeletal sites: Evidence for substantial trabecular bone loss in young adult women and men. J. Bone Miner. Res., 23: 205-214.

30. Meema, H.E., 1963. Cortical bone atrophy and osteoporosis as a manifestation of aging. Am. J. Roentgenol. Radium. Ther. Nucl. Med., 89: 1287-1295.
31. Anton, H.C., 1969. Width of clavicular cortex in osteoporosis. Br. Med. J., 1: 409-411.
32. Yao, J., Y. Liu, F. Chen, R.M. Summers and T. Bhattacharyya, 2013. Computer assisted measurement of femoral cortex thickening on radiographs. Proc. SPIE., Vol. 8670. 10.1117/12.2007605.
33. Morar, A., F. Moldoveanu, A. Moldoveanu, V. Asavei and A. Egner, 2010. Computer assisted analysis of orthopaedic radiographic images. Proceedings of the 9th WSEAS International Conference on Signal Processing, May 29-31, 2010, Catania, Italy, pp: 66-71.
34. Gluer, C.C., S.R. Cummings, A. Pressman, J. Li and K. Gluer, 1994. Prediction of hip fractures from pelvic radiographs: The study of osteoporotic fractures. J. Bone Miner Res., 9: 671-677.
35. Altman, D.G. and J.M. Bland, 1983. Measurement in medicine: The analysis of method comparison studies. J. Royal Statist. Soc. Series D: Statistician, 32: 307-317.
36. Riggs, B.L., S. Khosla and L.J. Melton III, 1998. A unitary model for involutional osteoporosis: Estrogen deficiency causes both type I and type II osteoporosis in postmenopausal women and contributes to bone loss in aging men. J. Bone Miner Res., 13: 763-773.
37. Anburajan, M., C. Rethinasabapathi, M.P. Korath, B.G. Ponnappa and T.M.R. Panicker *et al*., 2001. Low cost mass screening tool forevaluating post-menopausal osteoporosis: A breakthrough for the developing world. Bombay Hospital J., 43: 53-60.
38. Mather, J., J.C. MacDermid, K.J. Faber and G.S. Athwal, 2013. Proximal humerus cortical bone thickness correlates with bone mineral density and can clinically rule out osteoporosis. J. Shoulder Elbow Surg., 22: 732-738.
39. Hyldstrup, L. and S.P. Nielsen, 2001. Metacarpal index by digital X-ray radiogrammetry: Normative reference values and comparison with dual X-ray absorptiometry. J. Clin. Densitom., 4: 299-306.
40. Sapthagirivasan, V. and M. Anburajan, 2013. Diagnosis of osteoporosis by extraction of trabecular features from hip radiographs using support vector machine: An investigation panorama with DXA. Comput. Biol. Med., 43: 1910-1919.